Current Biology, Vol. 12, 13–25, January 8, 2002, ©2002 Elsevier Science Ltd. All rights reserved. PII S0960-9822(01)00632-7

Paraspeckles: A Novel Nuclear Domain

Archa H. Fox,[1] Yun Wah Lam,[1] Anthony K.L. Leung,[1] Carol E. Lyon,[1] Jens Andersen,[2] Matthias Mann,[2,3] and Angus I. Lamond[1,4]

[1] Wellcome Trust Biocentre
MSI/WTB Complex
University of Dundee
Dundee DD1 4HN
United Kingdom

[2] Department of Biochemistry and Molecular Biology
University of Southern Denmark
Campusvej 55
DK-5230 Odense M

[3] MDS Proteomics
Staermosegaadsvej 6
5230 Odense M
Denmark

Summary

Background: The cell nucleus contains distinct classes of subnuclear bodies, including nucleoli, splicing speckles, Cajal bodies, gems, and PML bodies. Many nuclear proteins are known to interact dynamically with one or other of these bodies, and disruption of the specific organization of nuclear proteins can result in defects in cell functions and may cause molecular disease.

Results: A proteomic study of purified human nucleoli has identified novel proteins, including Paraspeckle Protein 1 (PSP1) (see accompanying article, this issue of *Current Biology*). Here we show that PSP1 accumulates in a new nucleoplasmic compartment, termed paraspeckles, that also contains at least two other protein components: PSP2 and p54/nrb. A similar pattern of typically 10 to 20 paraspeckles was detected in all human cell types analyzed, including primary and transformed cells. Paraspeckles correspond to discrete bodies in the interchromatin nucleoplasmic space that are often located adjacent to splicing speckles. A stable cell line expressing YFP-PSP1 has been established and used to demonstrate that PSP1 interacts dynamically with nucleoli and paraspeckles in living cells. The three paraspeckle proteins relocalize quantitatively to unique cap structures at the nucleolar periphery when transcription is inhibited.

Conclusions: We have identified a novel nuclear compartment, termed paraspeckles, found in both primary and transformed human cells. Paraspeckles contain at least three RNA binding proteins that all interact dynamically with the nucleolus in a transcription-dependent fashion.

[4] Correspondence: a.i.lamond@dundee.ac.uk

Introduction

The nucleus is a complex organelle with an internal structure and component organization that is not fully characterized [1, 2]. Within the nucleus, protein and RNP complexes can move to and from chromatin through the interchromatin nucleoplasmic space, primarily by a diffusion mechanism [3, 4]. In addition, many nuclear factors are able to form or interact with different classes of subnuclear bodies, which are either attached to chromatin or located in the interchromatin space. These nuclear bodies, or "compartments," include nucleoli, splicing speckles, Cajal bodies, gems, and PML bodies [5]. They are not enclosed by membranes, yet are distinct from the surrounding nucleoplasm and contain proteins involved in different nuclear activities, such as ribosome biogenesis, transcription, and RNA splicing. Further, many observations indicate that the accurate maintenance of subnuclear organization has important consequences for cellular function [6–14].

There is increasing evidence that the internal organization of the nucleus and many of the protein and RNP factors within it are highly dynamic. The recent use of photobleaching techniques to analyze GFP-tagged proteins expressed in live cells has shown that nuclear proteins can diffuse rapidly and traffic at high rates between separate compartments [15–18]. The nuclear localization pattern of many proteins and, as a consequence, the overall structure of the nucleus has been shown to change during the cell cycle and in response to changes in cellular metabolic activity. For example, inhibiting transcription with drugs such as Actinomycin D, 5,6-dichloro-1-β-D-ribofuranosylbenzimadizole (DRB), or α amanitin all cause a significant redistribution of many nuclear factors and alter the morphologies of nucleoli and splicing speckles [19, 20].

Recent studies have started to provide clues concerning the specific roles of individual forms of nuclear bodies. The interchromatin granule clusters (speckles) that contain snRNPs and other spliceosome components may be sites for storage or recycling of splicing factors, although in some cases they may also be more directly involved in the splicing mechanism [21–23]. Cajal bodies specifically accumulate snRNPs and nucleolar snoRNPs that have recently been imported into the nucleus and are likely undergoing maturation [24–27]. Cajal bodies may have a role in RNA modification and transport and may also be involved in the feedback regulation of gene expression from snRNA gene loci [28]. In the case of nucleoli, it is known that they are sites for the transcription of rRNA genes and the subsequent processing of rRNA precursors and assembly of ribosomal subunits. Interestingly, there is also evidence that nucleoli may perform additional nuclear functions, such as controlling the activity of regulatory molecules by a sequestration mechanism and participating in the biogenesis of other RNP complexes [29–31].

The ability to purify large quantities of relatively pure nucleoli makes it an ideal candidate for biochemical

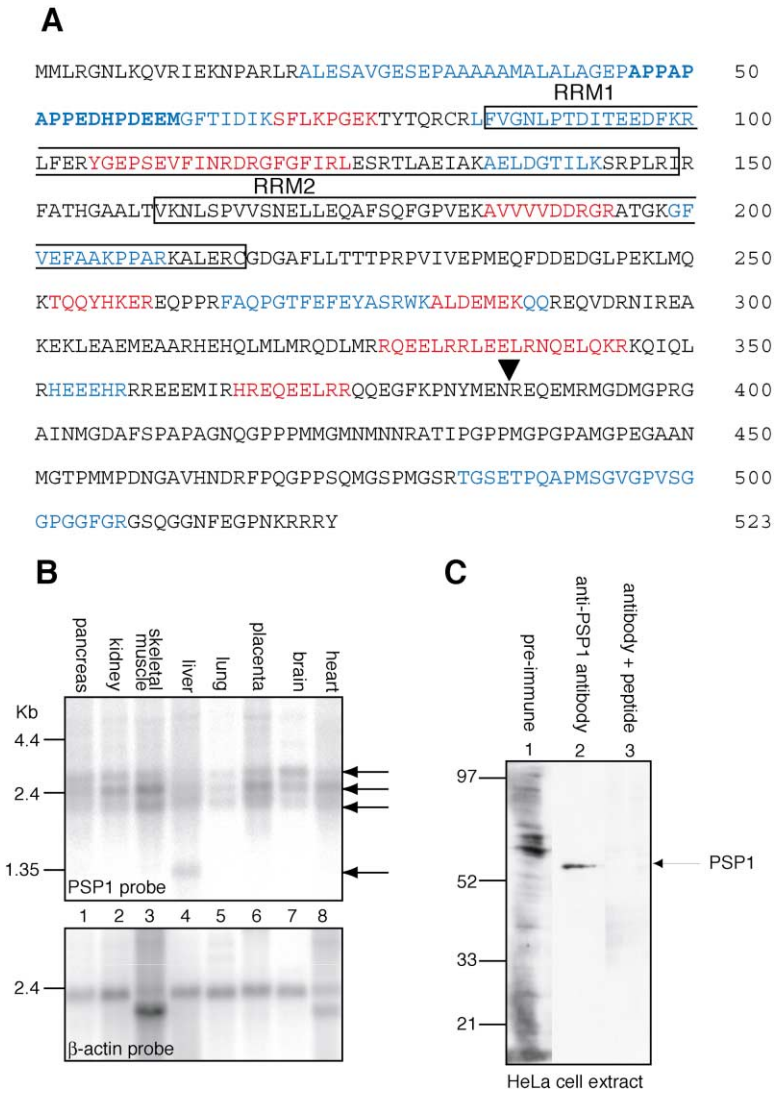

Figure 1. The Sequence and Expression of Paraspeckle Protein 1

(A) Amino acid sequence of PSP1. Prepublication accession numbers for PSP1: Genbank FLJ10955 and ENSEMBL gene ID ENSG00000121390. The arrowhead after residue 386 indicates the final common residue for both splice forms of PSP1. The shorter form (PSP1-β) has an additional 7 residues (GDKRKCG, a translation of exon 7), making it a total of 393 residues long. The remaining residues C-terminal to the arrowhead are the extent of the longer splice variant PSP1-α (523 residues long), composed of exons 8 and 9 as defined by the genomic annotation. Red and blue text indicates tryptic peptides identified using MS on PSP1 copurified with HeLa nucleoli. For further details of PSP1 splice forms, see Supplementary Material. The peptide at the N-terminus of PSP1 that the PSP1 antibody was generated against is shown in bold; this sequence is in a region of the protein with low similarity to p54/nrb and is thus unique to PSP1. The RNA-binding domains are boxed.

(B) Human Northern blot probed for PSP1. A human multitissue Northern blot (Clontech) was hybridized with a ^{32}P-radiolabeled cDNA probe for PSP1 (see Experimental Procedures) (upper panel), then stripped and reprobed with a β-actin probe to show approximately equal loading of mRNA in each lane (lower panel), as per the manufacturer's instructions. The hybridized radioactivity was visualized using a Phosphoimager. Tissue sources for the mRNA in each lane are indicated on the figure. We note that the signal for the PSP1 probe was considerably weaker than for the β-actin probe, possibly indicating that this is a low-abundance transcript.

(C) PSP1 protein in HeLa extract. HeLa cells were lysed and the resultant extract subjected to SDS/PAGE and transfer to nitrocellulose. The blot was divided into three and probed as follows: rabbit preimmune serum (PI) (lane 1), anti-PSP1 antiserum (lane 2), or anti-PSP1 antiserum preincubated with a 10 molar excess of cognate peptide (lane 3). These treatments were followed by incubation with HRP-conjugated anti-rabbit antibody and detection by chemiluminescence using ECL plus substrate (Amersham Pharmacia Biotech). The arrow indicates the major band of ~60 kDa in size that is detected specifically by the anti-PSP1 antiserum.

analysis in vitro. A major proteomic analysis of nucleoli isolated from cultured human cells has therefore been undertaken to characterize the protein composition of this important subnuclear body [32]. This study identified 271 human nucleolar proteins using MS, including 80 proteins encoded by novel or uncharacterized human genes. Here we report the characterization of one of the novel human nucleolar factors—Paraspeckle Protein 1 (PSP1). We show that PSP1 accumulates within a new form of nuclear compartment in the interchromatin space, termed paraspeckles. This analysis reveals a new level of structural complexity within the nucleus and highlights the dynamic nature of nuclear body proteins.

Results

PSP1: A Novel Protein from the Human Nucleolar Proteome that Localizes to a Punctate Pattern in the Nucleus

PSP1 was initially chosen for detailed analysis because we observed that it belonged to a subset of human nucleolar proteins that were enriched in nucleoli isolated from cells treated with the transcription inhibitor Actinomycin D [32]. Based upon a combination of cDNA sequence analysis and direct mass spectrometric identification of tryptic peptides, we deduce that the major form of PSP1 is a basic protein of 523 amino acids with a predicted Mr of 58.7 kDa (Figure 1A). As judged by probing a human multitissue Northern blot, PSP1 is encoded by several ubiquitously expressed mRNAs of ~2.5 kb, including alternatively spliced forms (Figure 1B). We have named the two major expressed isoforms PSP1-α and PSP1-β (see Figure 1 and Supplementary Material available with this article online). The primary amino acid sequence of PSP1 contains two conserved RNA binding domains (RRMs) located at the amino terminus of both isoforms and is most closely related to the nuclear protein p54/nrb [33, 34]. PSP1 is highly conserved in mammals, with a mouse ortholog showing greater than 95% identity at the amino acid level (Genpept accession number BAB27509). However, in lower organisms it is difficult to define clear orthologs, be-

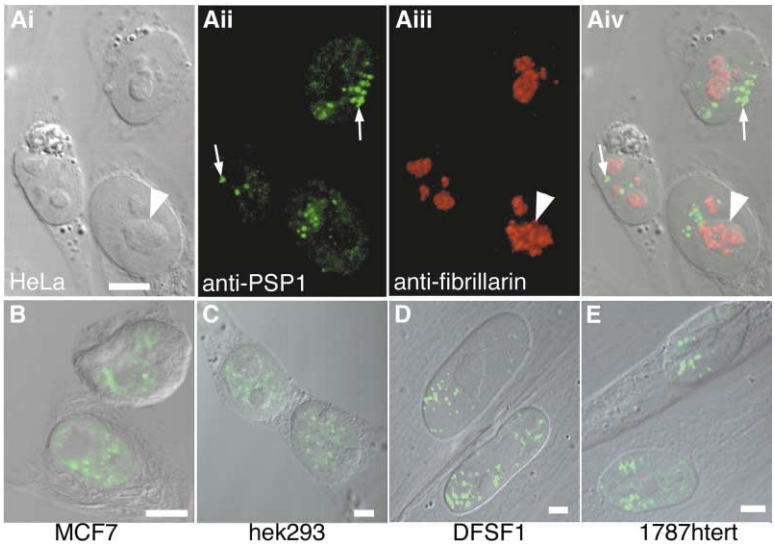

Figure 2. PSP1 Has a Punctate Nuclear Localization in Human Cells

The confocal fluorescence micrographs show PSP1 antiserum staining in the transformed cell lines (A) HeLa, (B) MCF7, (C) Hek293, and in the "primary" (D) DFSF1 and (E) 1787htert cells. An overlay of the Nomarski image for each cell type and the PSP1 immunostaining is shown in (B)–(E). The HeLa cells in (A) have also been immunostained using anti-fibrillarin antiserum (shown in panel [Aiii]), and the overlay of the Nomarski image for the cells as well as the fibrillarin and PSP1 signals is shown in panel (Aiv). Each fluorescent image is a stack of confocal sections. Arrowheads indicate nucleoli as seen in Nomarski and fibrillarin staining, and arrows indicate punctate PSP1 spots. Scale bars, 5 μm.

cause similar proteins appear to be equally divergent with both PSP1 and p54/nrb in *D. melanogaster* and *C. elegans*.

To analyze the cellular localization of PSP1, a rabbit polyclonal antibody was generated against a unique peptide sequence located near the amino terminus (shown bold in Figure 1A). The resulting antiserum was affinity purified using the cognate peptide and both the preimmune and affinity-purified sera used to detect HeLa proteins that had been separated by SDS-PAGE and transferred to a nitrocellulose membrane (Figure 1C, lanes 1 and 2). The preimmune serum showed only nonspecific binding (lane 1). In contrast, the affinity-purified antiserum predominantly detected a major band of ~60 kDa (lane 2), corresponding to the predicted size of PSP1-α, the longer isoform of PSP1. Longer exposure of the membrane revealed an additional band of the expected size for the smaller PSP1 isoform, PSP1-β (data not shown). The specific PSP1 bands were no longer detected when the affinity-purified antiserum was preblocked with the PSP1 peptide (lane 3).

Having established the specificity of the anti-PSP1 serum, we used it for indirect immunofluorescence staining of HeLa cells (Figure 2A). The anti-PSP1 antiserum specifically labeled HeLa nuclei in a punctate pattern, with some diffuse nucleoplasmic labeling (arrows in Figures 2Aii and 2Aiv). Surprisingly, although PSP1 was identified through proteomic analysis of nucleoli, the anti-PSP1 antiserum did not label nucleoli significantly, as shown by double-labeling experiments using an anti-fibrillarin antibody to detect nucleoli (Figures 2Ai, 2Aiii, and 2Aiv). The anti-PSP1 antiserum typically labeled instead 10 to 20 bright punctate structures scattered throughout the nucleoplasm.

The anti-PSP1 antiserum also labeled a similar pattern of punctate, nucleoplasmic structures, with varying levels of diffuse nucleoplasmic labeling but no significant nucleolar staining, in both primary and transformed human cell lines (Figures 2B–2E). These included transformed lines derived from either breast (MCF7, Figure 2B) or kidney cells (hek293, Figure 2C) and primary cells corresponding to foreskin fibroblasts (DFSF1, Figure 2D) or human fibroblasts extended in proliferative life span by retroviral expression of telomerase reverse transcriptase (1787htert, Figure 2E).

Tagged PSP1 Shows the Same Punctate Localization as Endogenous PSP1

To confirm that the punctate nuclear staining pattern observed with anti-PSP1 antiserum in primary and transformed human cells genuinely reflected the localization of PSP1, we transiently expressed exogenous PSP1 in HeLa cells fused with either a yellow fluorescent protein (YFP), or myc peptide tag (Figure 3). Both tagged forms of PSP1 showed a similar pattern to that seen with the anti-PSP1 antiserum in untransfected cells, including bright punctate nuclear structures. The tagged proteins did not accumulate in nucleoli, as detected by either DIC microscopy or immunolabeling with an anti-fibrillarin antibody (Figures 3A and 3B; arrowheads denote nucleoli; arrows denote tagged PSP1).

We next established stable HeLa cell lines expressing YFP-PSP1 (Figure 4). Separate cell lines were isolated for the two predominant splice forms of PSP1. As both isoforms gave identical results, subsequent data are presented only for the PSP1-β isoform. Immunolabeling both the parental and HeLa$^{YFP\text{-}PSP1\text{-}\beta}$ cell lines with anti-PSP1 antiserum detected a similar pattern of punctate, nucleoplasmic structures and diffuse nucleoplasmic staining (Figure 4, cf. panels 4Aiii and 4Biii). Analysis of 50 labeled cells from both the parental and stable cell lines showed that there was no statistical difference in the average number of punctate PSP1 structures labeled with PSP1 antiserum or YFP fluorescence (~15 per nucleus, data not shown; for example, Figure 4, panels 4Bii and 4Biii).

Proteins from both the parental and HeLa$^{YFP\text{-}PSP1\text{-}\beta}$ cells were separated by SDS-PAGE, transferred to nitrocellulose membrane, and probed with either anti-GFP (Figure 4C, lanes 1 and 2) or anti-PSP1 antiserum (Figure 4C, lanes 3–6). A single band was detected with the anti-GFP antibody specifically in the HeLa$^{YFP\text{-}PSP1\text{-}\beta}$ cells (lane 2). In contrast, the major endogenous PSP1 band was detected in both cell lines using the anti-PSP1 antiserum

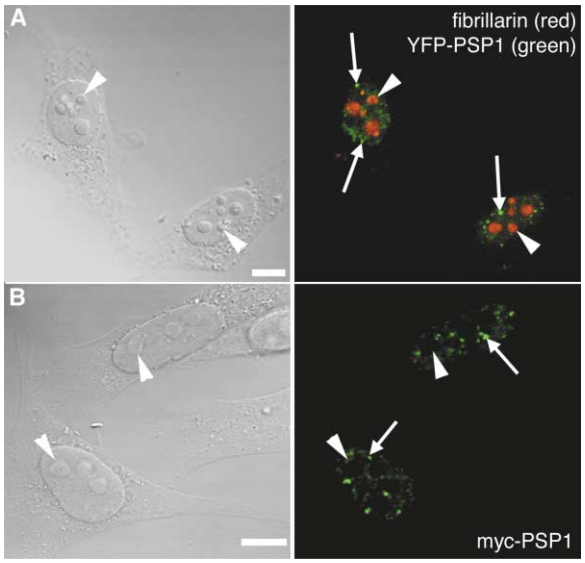

Figure 3. Tagged PSP1 Localizes to Punctate Foci in HeLa Nuclei

Confocal fluorescence micrographs are shown on the right, with the corresponding Nomarski images to the left. HeLa cells were transiently transfected with YFP-PSP1 (A) or myc-PSP1 (B) and fixed 16 hr after transfection. Panel (A) shows direct fluorescence of the YFP-PSP1 protein (green) and immunofluorescence staining for fibrillarin (red). Panel (B) shows HeLa nuclei immunostained with anti-myc antiserum (green). Large arrowheads indicate nucleoli, and arrows indicate the punctate YFP-PSP1 and myc-PSP1. Scale bars, 5 μm.

(lanes 3 and 4) but was absent when the antiserum was preblocked with the cognate peptide (lanes 5 and 6). We observe that the YFP-PSP1 fusion protein is expressed at ~4-fold higher levels than the endogenous PSP1 protein in HeLa$^{YFP\text{-}PSP1\text{-}\beta}$ cells (Figure 4C, lane 4 and other data not shown). However, the relative level of endogenous PSP1 appears higher in the parental cell line, suggesting that some degree of downregulation of endogenous PSP1 may have occurred to compensate for expression of the fusion protein (Figure 4C, cf. lanes 3 and 4).

We compared the physical properties of the endogenous and YFP-tagged PSP1 proteins in the parental and HeLa$^{YFP\text{-}PSP1\text{-}\beta}$ cell lines (Figure 4D). Cultured cells were extracted sequentially with buffers containing varying concentrations of salt and detergent, and the resulting protein samples were separated by SDS-PAGE, transferred to nitrocellulose, and probed with anti-PSP1 antiserum. In both the parental and stable cell lines, PSP1 was quantitatively recovered in the second fraction (Figure 4D, lanes 2 and 6). Furthermore, both the YFP-tagged and endogenous PSP1 were recovered in the same fraction from the HeLa$^{YFP\text{-}PSP1\text{-}\beta}$ cells (Figure 4D, lane 6). Thus, the tagged and endogenous PSP1 proteins have similar properties. Further comparison of the parental and HeLa$^{YFP\text{-}PSP1\text{-}\beta}$ cell lines showed no apparent change in their respective viability or rate of cell division (data not shown). We therefore conclude that the HeLa$^{YFP\text{-}PSP1\text{-}\beta}$ cell line is viable and expresses a single tagged YFP-PSP1 fusion protein that has a similar localization pattern and physical properties to the endogenous PSP1.

PSP1 Localizes in a Novel Nuclear Compartment

We next sought to identify which of the known subnuclear compartments PSP1 was accumulated in. Therefore, double-labeling experiments were carried out using the HeLa$^{YFP\text{-}PSP1\text{-}\beta}$ cell line to detect PSP1 and immunolabeling with characterized antisera to detect marker proteins for separate nuclear bodies (Figures 5A–5D). Antibodies specific for snRNPs (anti-2,2,7-trimethylguanosine-cap structure) and for the non-snRNP splicing factor SC35 were both used to detect splicing speckles (Figures 5A and 5B). We observed no overlap in the localization of PSP1 and splicing speckles using either of these antibodies (Figures 5Aiii and 5Biii; in each panel, arrows indicate YFP-PSP1, and arrowheads indicate known nuclear markers, e.g., speckles). The brighter foci detected with the snRNP marker also did not colocalize with YFP-PSP1 (Figures 5Aii and 5Aiii, broken arrows indicate bright foci). It is most likely that these bright snRNP foci represent Cajal bodies [20]. A double-labeling experiment with anti-coilin antiserum (a marker for Cajal bodies) confirmed that there is no overlap or colocalization with YFP-PSP1 (Figure 5Ciii). We also detected no colocalization of YFP-PSP1 either with the bodies labeled using an anti-SMN antiserum, which detects both Cajal bodies and gems [9] (data not shown), or with an anti-U1A antibody, which should label interchromatin granule associated zones [35] as well as speckles (data not shown). The other major class of subnuclear bodies that have been studied contain the cellular RING finger protein PML [6–8, 36]. Double labeling using an anti-PML antiserum showed that the YFP-PSP1 signal also does not localize or associate with PML bodies (Figure 5Diii). We next compared the localization of YFP-PSP1 with the major sites of RNA synthesis, as detected by pulsed incorporation of Br-UTP (Figure 5E). Despite the extensive nucleoplasmic labeling detected with the anti-BrdUTP antiserum, we again observed no obvious colocalization with the punctate YFP-PSP1 signal (Figure 5Eiii).

Finally, we used a triple-labeling protocol to compare the localization of YFP-PSP1 with both bulk chromatin, as detected by DAPI staining, and splicing speckles, as detected using anti-SC35 antiserum (Figure 6). This showed that the YFP-PSP1 localized predominantly to interchromatin regions that have little or no DAPI signal (Figure 6, DAPI-poor regions indicated by arrowheads). A similar result was obtained using a fluorescently tagged histone H2B and the anti-PSP1 antiserum (data not shown). Interestingly, although we still detected no colocalization of YFP-PSP1 with the SC35 domains, which also localize to the interchromatin regions, analysis of optical z sections of the triple-labeled nuclei showed that the YFP-PSP1 structures were frequently juxtaposed beside SC35 speckles (Figure 6, lower panels; arrows indicate YFP-PSP1, and arrowheads indicate SC35 speckles in DAPI-poor regions).

In conclusion, PSP1 concentrates in a novel form of punctate subnuclear structure that localizes to the interchromatin space. Considering both the speckled appearance of the PSP1-containing structures and their frequent localization adjacent to SC35 speckles, we have termed this novel compartment “paraspeckles.”

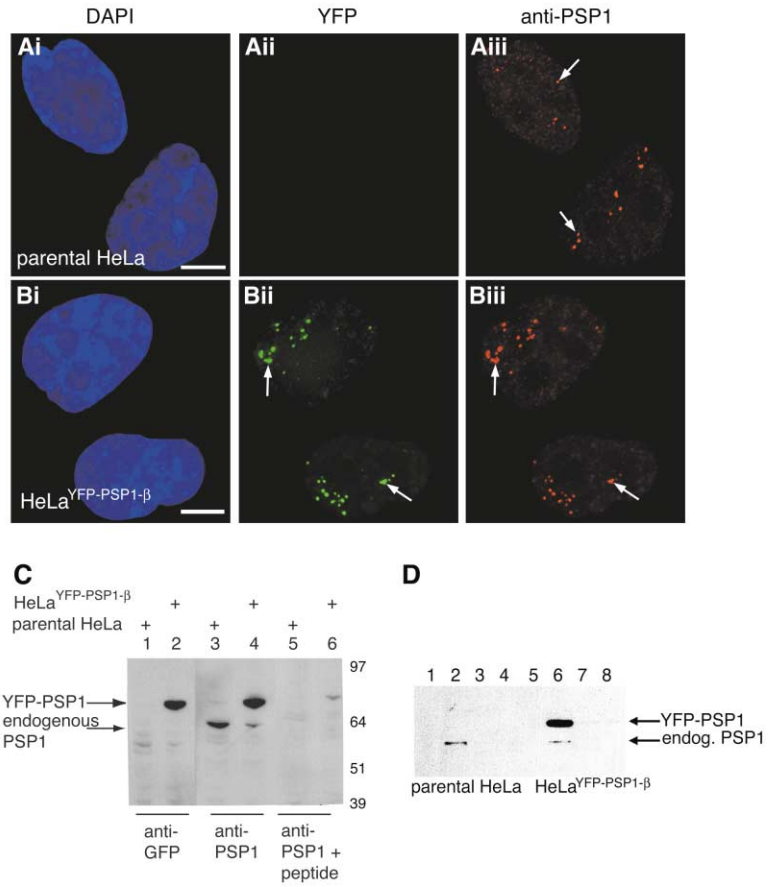

Figure 4. Stable Expression of YFP-PSP1 in HeLa Cells Results in the Same Punctate Pattern of PSP1 Localization in the Nucleus

Fluorescent micrographs of HeLa (A) and HeLa$^{YFP\text{-}PSP1\text{-}\beta}$ (B). The extent of the nucleus is shown with DAPI staining in panels (Ai)–(Bi), the fluorescence from the exogenously expressed YFP-PSP1 in panels (Aii)–(Bii), and the staining pattern for endogenous PSP1 as determined by staining with anti-PSP1 antiserum in panels (Aiii)–(Biii). All images are maximum intensity projections of stacks deconvolved using the deltavision Softworx software. Arrows point to examples of the same foci detected with the PSP1 antibody as appear in the YFP fluorescence channel. Scale bars, 5 μm. (C) Anti-PSP1 antiserum recognizes both the endogenous and fusion PSP1 proteins, while anti-GFP antiserum only recognizes YFP-PSP1. Equal amounts of HeLa cell extract (lanes 1, 3, and 5) and HeLa$^{YFP\text{-}PSP1\text{-}\beta}$ stable cell extract (lanes 2, 4, and 6) were electrophoresed, transferred to nitrocellulose, then immunoblotted with anti-GFP antibody (lanes 1 and 2), anti-PSP1 antibody (lanes 3 and 4), or anti-PSP1 antibody preblocked by incubation with 10-fold excess of cognate peptide (lanes 5 and 6). An anti-rabbit peroxidase conjugated secondary antibody was employed to detect antibody binding, and this in turn was detected using ECL plus (Amersham Pharmacia Biotech). (D) Biochemical behavior of endogenous PSP1 and YFP-PSP1. HeLa$^{YFP\text{-}PSP1\text{-}\beta}$ cells (samples in lanes 5–8) and parental HeLa cells (samples in lanes 1–4) were both extracted in several buffers containing different concentrations of salts and detergents (see Experimental Procedures). Equivalent protein samples from each sequential extract were loaded onto a gel, electrophoresed, transferred to nitrocellulose, and immunoblotted with anti-PSP1 antibody. The following extracts were loaded in each lane: supernatant A (lanes 1 and 5), supernatant B (lanes 2 and 6), supernatant C (lanes 3 and 7), and pellet C (lanes 4 and 8). Both endogenous and YFP-PSP1 are specifically released from the YFP-PSP1 cells in supernatant B (lane 6), and the endogenous PSP1 from parental HeLa is also specifically released in supernatant B (lane 2). Arrows indicate endogenous PSP1 and exogenous YFP-PSP1 proteins.

PSP1 Relocalizes to the Nucleolus When Transcription Is Blocked

We next examined how the localization of PSP1 was affected by ongoing gene expression, which is known to alter the structure of other subnuclear bodies. After treatment of the HeLa$^{YFP\text{-}PSP1\text{-}\beta}$ cell line with Actinomycin D, which halts elongation by RNA polymerases, we observed a dramatic reorganization of PSP1 from a pattern of paraspeckles to discrete caps formed at the nucleolar periphery (Figure 7A, cf. panels 7Ai and 7Aii). This response contrasts with the behavior of splicing speckle proteins, which concentrate in enlarged speckles in the nucleoplasm after Actinomycin D treatment, as shown here for SC35 (Figure 7Aiii and 7Aiv; arrows indicate PSP1, and arrowheads indicate SC35). A similar effect was observed upon treating cells with a separate inhibitor of RNA synthesis, DRB, indicating that it most likely results from an inhibition of transcription (data not shown). Analysis of PSP1 localization in a live HeLa$^{YFP\text{-}PSP1\text{-}\beta}$ cell at multiple time points after addition of Actinomycin D to the culture medium showed a progressive loss of PSP1 signal from nucleoplasmic paraspeckles and a concomitant appearance of PSP1 signal at the nucleolus (Figure 7B). We never observed the direct movement of whole paraspeckles to the nucleolus, suggesting that the PSP1 protein can flux out of the paraspeckles and accumulate at a separate nuclear location when transcription is inhibited.

The data above are consistent with the proteomic analysis of nucleoli, which showed that a subset of 11 proteins, including PSP1, was enriched in nucleoli following treatment of cells with Actinomycin D [32]. We asked if any of these 11 proteins shared a paraspeckle localization with PSP1. However, for most of these enriched proteins, previous studies have reported that they localize to known nuclear structures [37–40]. For example, our analysis of YFP-tagged p68 and p72 showed that they did not localize to paraspeckles (data not shown) but rather displayed a diffuse punctate nucleoplasmic pattern as previously described [38]. However, transient expression of YFP-tagged p54/nrb, the most closely related PSP1 homolog, showed that it was also a paraspeckle protein as judged by double labeling with the anti-PSP1 antiserum (data not shown). Interestingly, another novel protein identified in the proteomic study

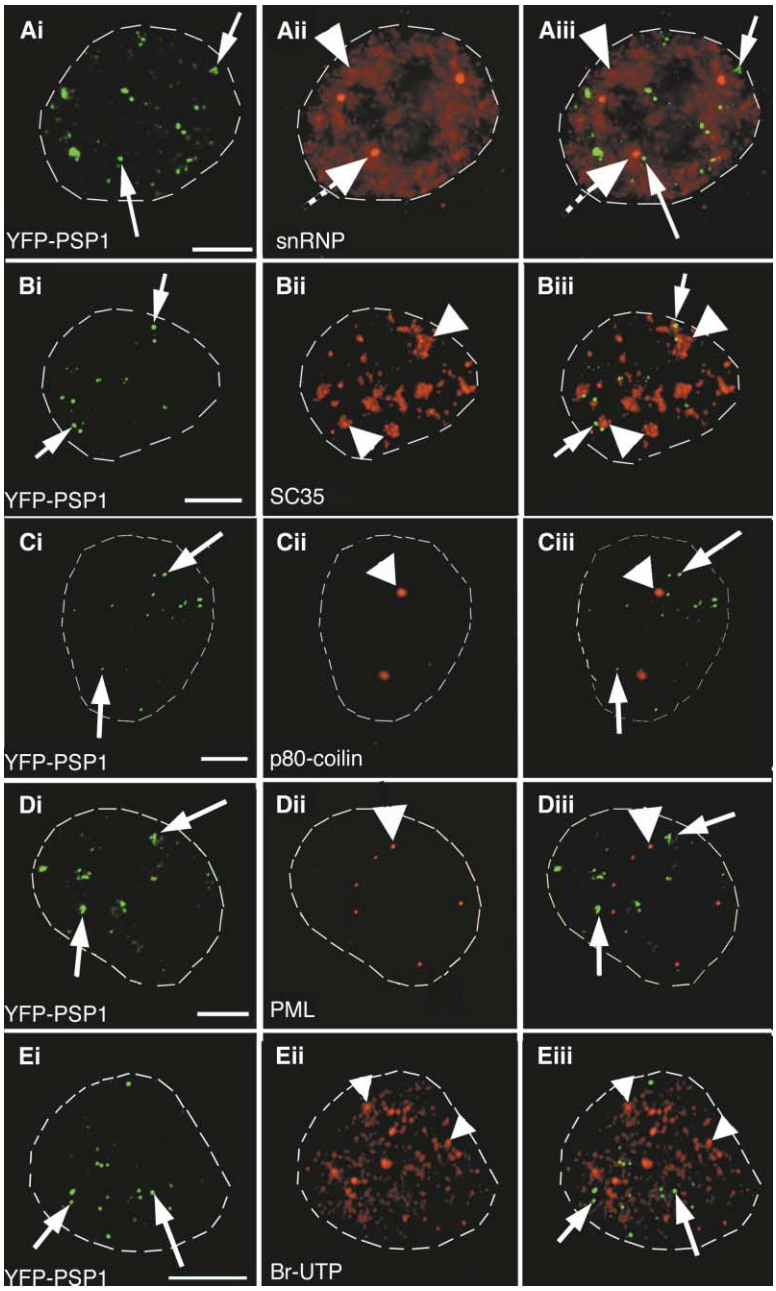

Figure 5. PSP1 Localizes to a Novel Subnuclear Compartment

HeLa$^{YFP\text{-}PSP1\text{-}\beta}$ cells were fixed and immunostained with antibodies against nuclear markers (red, panels [Aii]–[Dii]), the YFP-PSP1 fluorescence is shown in green in panels (Ai)–(Ei), and the overlay in panels (Aiii)–(Eiii). The following proteins were labeled: (A) snRNP splicing speckles as defined by staining with anti-5′-trimethylguanosine antiserum, (B) SC35 splicing speckles, (C) p80-coilin labeling Cajal bodies, and (D) PML labeling PML bodies. In (E), the transcription sites in HeLa$^{YFP\text{-}PSP1\text{-}\beta}$ cells were labeled using Br-UTP incorporation, followed by detection with anti-BrdUTP antiserum (panel [Eii]), and the overlay is shown in panel (Eiii). Each panel shows maximum intensity projections of deconvolved sections acquired using a deltavision system. The nuclei are outlined with hand-drawn dashed lines to indicate the nuclear periphery. Scale bars, 5 μm. Large arrowheads indicate the known nuclear structures, broken arrows indicate Cajal bodies in panels (Aii) and (Aiii), and small arrows indicate YFP-PSP1 foci.

as enriched in nucleoli from Actinomycin D-treated cells also localized to paraspeckles and therefore has been named "PSP2" (Figure 7C). Unlike p54/nrb, PSP2 shows minimal homology to PSP1, although it also contains two amino-terminal RNA binding domains. Transient expression of YFP-tagged PSP2 and double labeling with anti-PSP1 antiserum revealed that it accumulates in paraspeckles and shows diffuse nuclear staining and, like PSP1, also relocalizes to perinucleolar caps following Actinomycin D treatment (Figure 7C). Furthermore, all three paraspeckle proteins, i.e., PSP1, PSP2, and p54/nrb, colocalize in the same perinucleolar caps after Actinomycin D treatment (data not shown).

Other nuclear proteins, including fibrillarin and p80 coilin, are also known to relocalize into perinucleolar caps following treatment of cells with transcription inhibitors [20, 32, 41, 42]. We therefore performed triple-labeling experiments in Actinomycin D-treated HeLa$^{YFP\text{-}PSP1\text{-}\beta}$ cells with anti-p80 coilin and anti-fibrillarin antibodies (Figure 7D). This showed that all three proteins localize to different and distinct cap structures at the nucleolar periphery (Figure 7Div).

The twin observations that PSP1 can be detected, albeit in low amounts, in purified nucleoli and that it becomes enriched in nucleoli after Actinomycin D treatment ([32] and this study, Figure 7A), suggest the possibility that it cycles continually between paraspeckles and the nucleolus. To add support to this hypothesis,

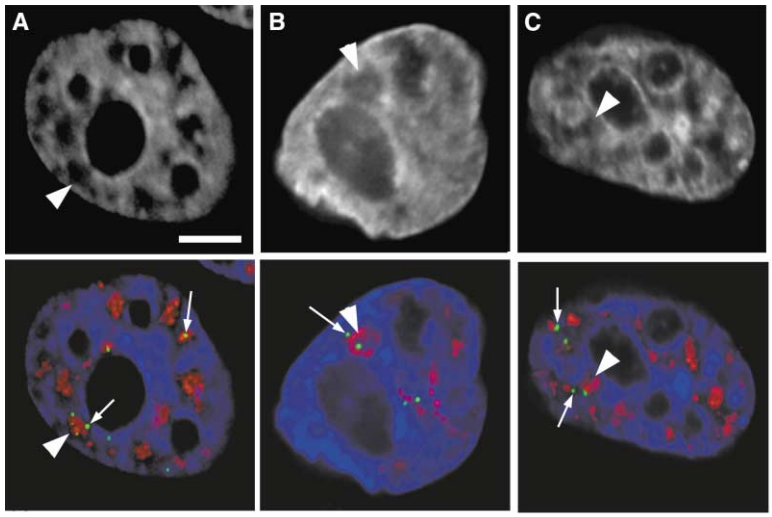

Figure 6. Paraspeckles Are Found in Interchromosomal Spaces, Often Next to SC35 Speckles

Upper panels indicate single sections through three representative HeLa$^{YFP\text{-}PSP1\text{-}\beta}$ nuclei (A–C) stained with DAPI to highlight chromatin. The arrowheads indicate the DAPI-poor staining interchromosomal regions. The lower panels show DAPI staining (blue), YFP-PSP1 fluorescence (green), and SC35 immunostaining (red) from the same sections from the same nuclei as shown in the upper panels. The sections were obtained using the Deltavision system and the images were deconvolved using Softworx. Small arrows indicate paraspeckles, and arrowheads indicate SC35 clusters that reside within the dark, low-stained DAPI areas. Scale bar, 5 μm.

we performed a fluorescence loss in photobleaching (FLIP) experiment, using the HeLa$^{YFP\text{-}PSP1\text{-}\beta}$ cell line, to see if photobleaching of the nucleolus affects the fluorescence signal of YFP-PSP1 in paraspeckles (Figure 8). Several cells were imaged over the course of the experiment, while pulse photobleaching a region of interest inside the nucleolus of one cell only. The nucleoplasmic fluorescence of the cell in which the nucleolus was bleached decreased over the time course of the experiment, as compared with the unbleached cell (Figure 8A). This indicates that nucleoplasmic PSP1 was moving into the nucleolus where it became subject to bleaching. We measured the fluorescence intensity of the individual paraspeckles within the bleached cell and compared this with paraspeckles from an adjacent, unbleached control cell (Figure 8B). This showed a sequential loss of fluorescence in the paraspeckles of the cell in which the nucleolus was bleached. We conclude that the most likely explanation of this result is that PSP1 cycles between the paraspeckles and nucleolus.

Discussion

We have identified in this study a novel nuclear compartment (paraspeckles) and shown that at least three nuclear proteins, i.e., PSP1, PSP2, and p54/nrb, accumulate in these structures. The paraspeckles were detected in both primary and transformed human cell lines and are different from other well-characterized types of subnuclear bodies. They are dynamic structures containing proteins that can cycle to and from nucleoli. The identification of paraspeckles underlines the high degree of organization of nuclear factors and the potential to segregate proteins within the nucleoplasm into biochemically and spatially distinct structures.

Considering that PSP1 was first identified using MS as a nucleolar factor [32], it was initially surprising that localization studies did not detect it accumulated in nucleoli. However, as reported above, it is likely that PSP1 cycles between paraspeckles and nucleoli, thus explaining its detection in nucleolar preparations by MS. The fact that proteins that may interact dynamically or transiently with nucleoli were nonetheless detected by MS analysis illustrates the utility of large-scale proteomic analyses of purified cellular structures. Furthermore, the MS data showing that PSP1, PSP2, and p54/nrb are all members of a group of proteins enriched in nucleoli isolated from Actinomycin D-treated cells also supports the fluorescence microscopy data in this study, showing that these proteins accumulate at the nucleolar periphery when cells are exposed to Actinomycin D. While we have identified here three separate paraspeckle proteins, it may in the future be possible to use a proteomic approach to characterize the full range of proteins localized in paraspeckles if a suitable isolation procedure can be developed. In this regard, the recent report describing the identification of proteins associated with a purified interchromatin granule cluster (speckle) fraction from mouse liver cells [43] is encouraging for future efforts in purifying subnuclear bodies.

The present data show that the distribution patterns of the three paraspeckle proteins likely reflect steady state accumulations rather than static localizations, consistent with the dynamic behavior reported also for other nuclear factors (reviewed in [3, 4]). Using the HeLa$^{YFP\text{-}PSP1\text{-}\beta}$ cell line, we observed that photobleaching of nucleoli led to a progressive loss of the YFP-PSP1 signal from paraspeckles. Several recent studies have also reported the converse phenomenon, i.e., bleaching of the nucleoplasm leading to a loss of fluorescent signal for a variety of nucleolar proteins [15–17]. These data collectively reveal that, for both factors accumulated in nucleoli and factors in nucleoplasmic structures, a high level of exchange can occur between compartments. This emphasizes the importance of dynamic studies and time-lapse analyses in order to understand the significance of localization patterns revealed by fluorescence microscopy.

Although the nucleolus is known to be the site of rRNA synthesis and ribosomal subunit assembly, it has been suggested that nucleoli can also perform other functions [30, 31, 44]. In this regard it is interesting that we have detected three proteins with no known connection to

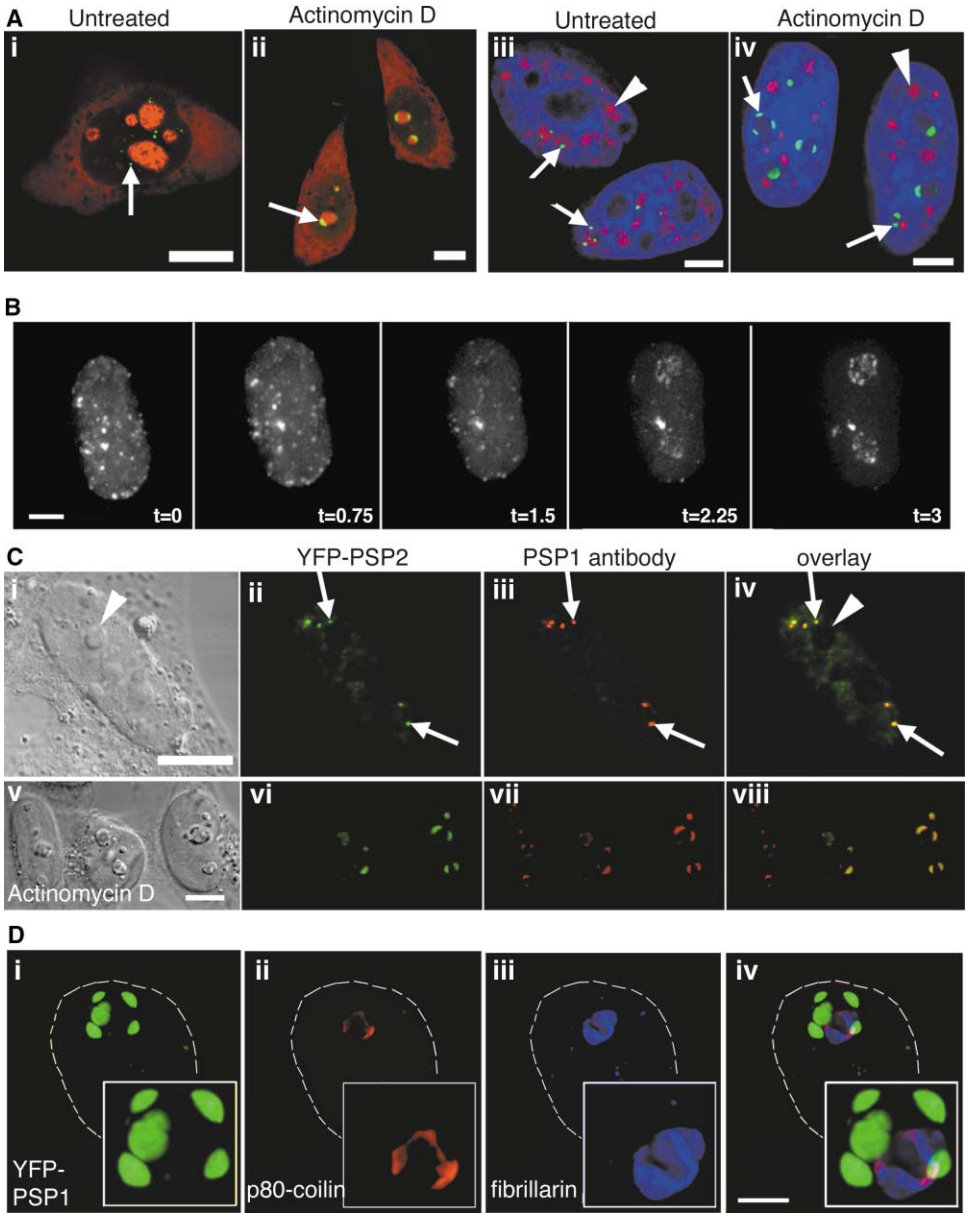

Figure 7. Inhibition of RNA Polymerase II Transcription Results in the Relocalization of PSP1 and Other Paraspeckle Proteins to the Nucleolus

(A) Fluorescence micrograph of sections through HeLa$^{YFP\text{-}PSP1\text{-}\beta}$ cells untreated (Ai and Aiii) and following incubation with media containing Actinomycin D (1 μg/ml) for 4 hr (Aii and Aiv). YFP-PSP1 fluorescence is shown in green in all panels. For other colors, panels (Ai) and (Aii) show cellular RNA (including nucleoli) by staining with Pyronin Y (red), and panels (Aiii) and (Aiv) show DNA as indicated by DAPI staining (blue) and SC35 as indicated by immunostaining with anti-SC35 antiserum (red). Small arrows indicate YFP-PSP1 paraspeckles and relocalized YFP-PSP1 at the nucleolar periphery. Arrowheads indicate SC35 clusters in untreated cells and relocalized SC35 enlarged speckles after treatment with Actinomycin D.

(B) PSP1 relocalizes in response to transcription inhibition in live cells. The panels show a series of time points demonstrating the gradual relocalization of PSP1 from paraspeckles to nucleoli from a movie of a live HeLa$^{YFP\text{-}PSP1\text{-}\beta}$ cell imaged following the addition of media containing 1 μg/ml Actinomycin D. The cell was imaged as described in Experimental Procedures, every 10 min over a 3 hr period.

(C) PSP2 is another paraspeckle protein. HeLa cells were transiently transfected with an expression vector for YFP-PSP2 and were fixed and immunostained using anti-PSP1 antiserum 16 hr later. Nomarski images of cells are shown in panels (Ci) and (Cv). The confocal fluorescence micrographs show YFP-PSP2 fluorescence in panels (Cii) and (Cvi), PSP1 immunostained signal in panels (Ciii) and (Cvii), and the overlays of the two channels are shown in panels (Civ) and (Cviii). Arrows indicate examples of the structures/paraspeckles that contain both PSP1 and PSP2. Panels (Ci)–(Civ) depict an untreated HeLa cell, while panels (Cv)–(Cviii) show HeLa cells that were incubated with Actinomycin D prior to fixation and immunostaining for PSP1. Note that one of the cells in panels (Cv)–(Cviii) does not have an YFP-PSP2 signal, presumably as it did not take up the expression plasmid in the transient transfection.

(D) Fibrillarin, coilin, and PSP1 are in distinct domains around the nucleolus when transcription is inhibited. Panels show a 3D reconstruction of a HeLa$^{YFP\text{-}PSP1\text{-}\beta}$ cell that has been fixed and immunostained for coilin (Dii) and fibrillarin (Diii) following incubation with Actinomycin D (1 μg/ml for 4 hr). YFP-PSP1 fluorescence is shown in (Di), and the overlay of the three signals is shown in (Div), note that, due to displaying a 3D structure in 2D, some artificial overlap of the colors is apparent. The insets in each panel are shown to more clearly demonstrate the distribution of the proteins around the nucleolar space. The images are 3D volume views of a stack of 60 × 0.2 μm sections deconvolved using the Softworx package. The nucleus is outlined with a hand-drawn dashed line. Scale bars, 5 μm.

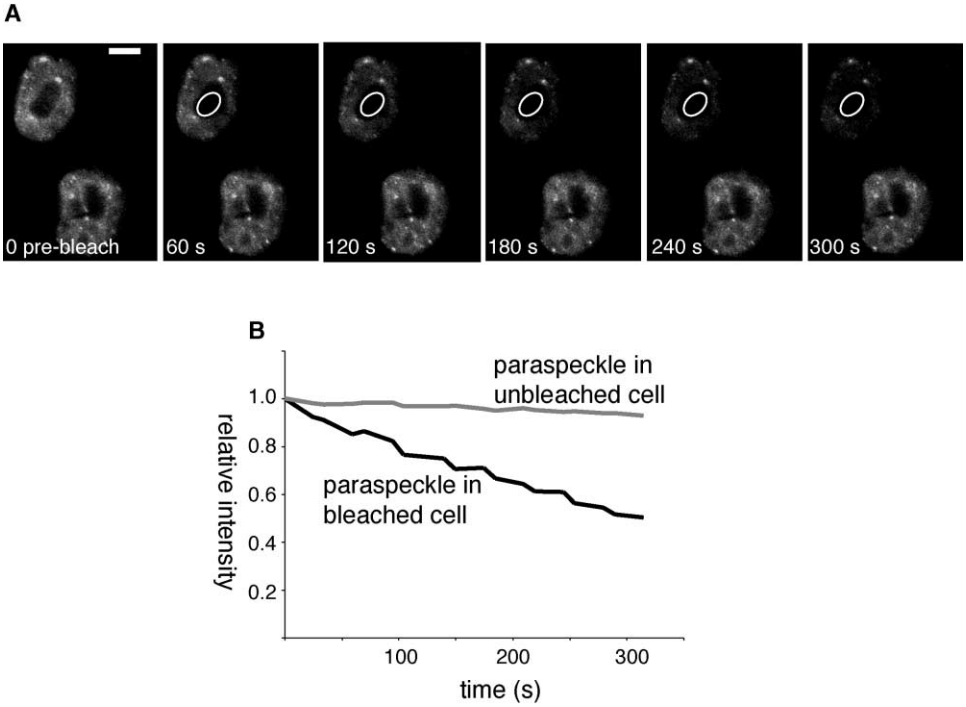

Figure 8. FLIP Experiments after Bleaching of Nucleoli in HeLa$^{YFP\text{-}PSP1\text{-}\beta}$ Cells Demonstrate that YFP-PSP1 Cycles between the Nucleolus and Nucleoplasmic Structures

(A) Following the acquisition of a prebleach image, a HeLa$^{YFP\text{-}PSP1\text{-}\beta}$ cell was periodically bleached inside the outlined area within the nucleolus. Images were collected before and after bleaching. The images shown here are time points occurring every minute for a 5 min experiment. The repeated bleach pulses do not affect a neighboring cell nucleus. Scale bar, 5 μm.

(B) Quantitation of changes in fluorescence intensity within selected paraspeckles in the bleached and unbleached cells (shown in [A]) over the course of a 5 min experiment.

ribosome biogenesis that associate with both nucleoli and paraspeckles. This may reflect that PSP1, PSP2, and p54/nrb have hitherto unknown roles in ribosome assembly or function or that the nucleolus is involved in other nuclear functions. Data from the proteomic analysis of purified nucleoli also raised the possibility of additional nucleolar functions [32]. PSP1 is a novel protein whose cellular function is not known. In the case of p54/nrb, previous studies have implicated it in multiple processes, including transcriptional regulation, splicing, apoptosis, and dsRNA processing [45–49]. In particular, p54/nrb has recently been implicated, in partnership with other proteins, in cotranscriptional control through an interaction with steroid hormone nuclear receptors [50]. Interestingly, despite being uncharacterized at the time of its identification in the nucleolar proteome, PSP2 has recently been identified independently and reported to be a "coactivator activator" (CoAA) that coactivates transcription by association with the thyroid hormone receptor binding protein [51]. These related functions of p54/nrb and PSP2, in combination with the data showing that paraspeckle proteins accumulate at nucleoli when transcription is inhibited, suggest a possible role for the paraspeckle proteins in transcriptional control and also implicate the nucleolus in these processes.

The fact that all three paraspeckle proteins contain related RNA binding domains suggests that their function may be connected to RNA metabolism. It will be interesting, therefore, to determine which RNA substrates PSP1 and PSP2 can interact with and to see whether any other protein components of the paraspeckles contain similar RNA binding motifs. However, we note that the PSP1 RNA binding motif is unlikely to be sufficient to target proteins to paraspeckles, because our preliminary data indicate that the RNA binding region of PSP1 alone is unable to cause accumulation of YFP in paraspeckles (data not shown). Both PSP1 and p54/nrb also show homology to the RNA binding and carboxy-terminal regions of the splicing factor PSF [37]. Like the paraspeckle proteins, PSF was identified by MS as one of the factors that accumulated in nucleoli after Actinomycin D treatment [32]. This is consistent with the recent report that GFP-tagged PSF relocalizes predominantly to perinucleolar clusters following Actinomycin D treatment [52]. However, unlike the paraspeckle proteins, PSF was reported to colocalize with splicing factors in the nucleus when transcription is active [37, 52]. Proteins in the PSP1 family may have roles in various aspects of nuclear organization concerned with RNA processing. For example, p54/nrb was recently isolated in a complex with PSF and matrin 3 (a putative component of the nuclear matrix) that bound and retained double-stranded inosine-containing RNA inside the nucleus [49]. Furthermore, a *C. tentans* protein, hrp65, which has ~36% identity with both the human PSP1 and p54/nrb proteins, localizes to fine fibers

that interact with Balbiani ring pre-mRNP particles inside the nucleoplasm of insect cells, as judged by electron microscopy [53]. Interestingly, hrp65 structures do not associate with pre-mRNA cotranscriptionally. Considering that paraspeckles are distinct from sites of Br-UTP incorporation in mammalian cell nuclei, it is possible these hrp65 fibers represent insect cell structures related to paraspeckles.

In addition to the major classes of subnuclear bodies that are shown here not to colocalize with paraspeckles, there have been reports of other types of punctate subnuclear structures that so far have been studied in less detail [54–61]. Although we have not compared these structures directly with paraspeckles, based upon their reported properties it seems unlikely that any of them correspond to paraspeckles. For example, unlike paraspeckles, YT bodies are not found in MCF7 cells and colocalize with sites of BrUTP incorporation [61], while the perinucleolar compartment (PNC) is not found in all cell types and is only present when transcription is active (reviewed in [62]). Nonetheless, we cannot exclude that some proteins that have been reported previously to have a punctate nuclear staining pattern may in future be shown to be components of paraspeckles.

It is unclear how and why, after inhibiting transcription, some nuclear proteins segregate into distinct perinucleolar cap structures (as seen in Figure 7D). Interestingly, the paraspeckle proteins all reside within the same nucleolar cap (and appear excluded from the coilin or fibrillarin caps). Further to this, we have observed that the DEAD box factors p68 and p72 (also found enriched in nucleoli isolated from cells treated with Actinomycin D [32]) also colocalize with PSP1 in perinucleolar caps following treatment of cells with Actinomycin D (data not shown, see Supplementary Material). Thus, p68 and p72 may be either functionally or biochemically related to the paraspeckle proteins.

In conclusion, we have identified a novel nucleoplasmic structure, termed paraspeckles, detected in all human cell types analyzed and shown to contain at least three separate proteins. These proteins appear to cycle continually between paraspeckles and the nucleolus, but all three accumulate in perinucleolar caps when transcription is inhibited. The prevalence of paraspeckles and their dynamic relationship to the nucleolus provides a new challenge for the ongoing effort to understand the functional complexity of nuclear structure.

Experimental Procedures

Plasmid Constructs and Antibody Production

The two main species of ESTs for PSP1 and thus the most often expressed forms corresponded to the two different PSP1 isoforms (PSP1-β residues 1–393) and (PSP1-α residues 1–523). To clone these, PSP1-β was amplified by PCR using the EST IMAGE 3634993 (UK HGMP Resource Centre), and PSP1-α was amplified using the overlapping templates EST IMAGE 2440134 and IMAGE 3634993. In both cases, the fragments were purified, digested with EcoRI and BamHI, and ligated into pEYFP-C1 (Clontech).

To make a myc-tagged fusion of PSP1, PSP1-β was amplified using IMAGE 3634993 as a template; the product was digested with BamHI and HindIII and subcloned into pSG9M [63]. YFP-p54/nrb was made by amplification of p54/nrb from a HeLa mRNA library (Clontech). The amplified product was digested with HindIII and BamHI and ligated into pEYFP-C1. YFP-PSP2 was made by amplification of the full-length cDNA constructed using the overlapping ESTs IMAGE 2350028 and 3505412. The resultant product was then digested with EcoRI and BamHI and ligated into pEYFP-C1.

For probing the multitissue Northern blot, a cDNA probe containing sequence corresponding to 107–702 bp of PSP1 was radiolabeled and purified prior to hybridization according to the manufacturer's instructions (Clontech).

An affinity-purified peptide antibody against PSP1 was generated in rabbit, using the sequence APPAPAPPEDHPDEEM (Eurogentec). This sequence was chosen as it lies within a region of PSP1 with little or no similarity with other proteins and is thus unique to PSP1.

Cell Culture and Transfection Assays, Generation of Stable Cell Line

HeLa cells, obtained from ATCC, were grown in Dulbecco's modified Eagle's medium (DMEM) supplemented with 10% fetal calf serum (FCS) and 100 U/ml penicillin and streptomycin (Life Technologies). For detection of fluorescent fusion proteins with fluorescence microscopy, cells were grown on coverslips and transfected with the appropriate construct, using Effectene reagent (Qiagen) according to the manufacturer's instructions. At 12–16 hr posttransfection, the cells were fixed for 7 min in 3.7% (w/v) paraformaldehyde in CSK buffer (10 mM PIPES [pH 6.8], 10 mM NaCl, 300 mM sucrose, 3 mM $MgCl_2$, 2 mM EDTA) at room temperature, mounted on to glass slides, and imaged under microscopes as described below. For both forms of YFP-PSP1 and the myc-PSP1 expression vectors, these were transient transfections. Thus, there was variation in the expression levels of the fusion proteins, resulting in variation in the number and intensity of PSP1 foci observed, with overexpressing cells showing numerous (>100) bright nuclear and cytoplasmic foci and with low expressors resembling the anti-PSP1 antiserum staining pattern. Thus, we concluded that the low-expressing pattern reflected the genuine localization of PSP1.

The YFP-PSP1 stable cell lines were generated essentially as described in [64]. These stable cells showed a pattern of YFP-PSP1 localization that resembled the low-expressing transiently transfected cells.

Drug treatments were carried out as follows: Actinomycin D (1 μg/ml) (Sigma) or DRB (100 μM) (Calbiochem) in DMEM incubated for 4 hr followed by fixation and fluorescence microscopy.

Preparation of Cell Lysates and Immunoblotting

Confluent 10 cm dishes of cells were washed with PBS and lysed using 1$\times$ LDS sample buffer (Novex). Lysates were passed through a Qiashredder (Qiagen) before being denatured using 100 mM DTT and heating at 70°C, then electrophoresed on a 1 mm, 4%–12% tris-glycine polyacrylamide gel (Novex) with MOPS buffer (Novex). Proteins were subsequently transferred onto nitrocellulose membrane (Schleicher and Schuell) using a submarine system (Novex) and buffer containing 12 mM Tris, 100 mM glycine, and 20% methanol. Following blocking with 5% milk powder in PBS + 0.05% Tween 20, the membranes were incubated with rabbit anti-PSP1 antibody (1:2000 dilution) or mouse anti-GFP antibody (Roche, 1:1000 dilution) detected using rabbit HRP conjugate (1:2000 dilution) or mouse HRP conjugate (1:5000 dilution) (both Pierce Chemical Co.) in PBS containing 5% milk powder and 0.05% Tween 20, and detected via chemiluminescence with ECL plus (Amersham Pharmacia Biotech).

Salt and detergent extraction of HeLa and HeLa$^{YFP\text{-}PSP1\text{-}\beta}$ cells was performed as described in [65]. Approximately equal amounts of protein were loaded in each lane, as estimated by Ponceau staining of proteins transferred to nitrocellulose membrane in pilot experiments. Samples were then subjected to immunoblotting as described above, with anti-PSP1 antiserum and anti rabbit HRP conjugate.

Immunofluorescence Microscopy

Cells were washed in PBS and fixed (as above) at room temperature. Permeabilization was performed with 1% Triton X-100 in PBS for 15 min at room temperature. Immunofluorescence staining was carried out using standard techniques. Antibodies used were anti-PSP1 rabbit peptide antibody (dilution 1:50), anti-fibrillarin monoclonal 72b9 (dilution 1:10, [66]), anti-myc monoclonal 9E10 (dilution 1:100,

[67]), anti-SC35 monoclonal (dilution 1:1000, Sigma), anti-2,2,7-trimethy-guanosine monoclonal (dilution 1:10, Calbiochem), anti-p80 coilin monoclonal 5P10 (dilution 1:10), anti-PML monoclonal PGM3 (dilution 1:10, Santa Cruz), anti-SMN monoclonal (dilution 1:50, Transduction Laboratories), and FITC and TRITC conjugated secondary antibodies (Jackson Laboratories). Transcription sites were visualized in live cells using previously described methods [68], and the resultant Br-UTP-containing mRNA was detected using anti-Bromo-dUTP antibody (dilution 1:5, Roche). Prior to mounting on slides, coverslips were sometimes soaked in DAPI (1 μM in water for 1 min) to stain DNA and/or followed by soaking in Pyronin Y (0.66 mM in water for 2 s) to stain RNA. Cells were mounted in either Mowiol/Dabco (for the confocal microscope) or 0.5% p-phenylenediamine in 20 mM Tris (pH 8.8), 90% glycerol (for the deltavision system).

Fluorescence microscopy of fixed cells was carried out using a 40× NA 1.3, 63× NA 1.4, or a 100× NA 1.4 Plan-Apochromat objective. Three-dimensional images and sections were recorded either on a LSM410 confocal microscope (Zeiss) or on a Zeiss DeltaVision Restoration microscope (Applied Precision, Inc.). Images presented here are projections of the entire nuclear fluorescence, unless otherwise stated.

Observation of Live Cells and Photobleaching Analysis

For live cell imaging, cells were grown on 42 mm glass coverslips (no. 1; Helmut Sauer) in medium containing 200 μg/ml G418. Cells were maintained at 37°C by use of a closed perfusion chamber (Bachofer) in DMEM media without phenol red (Life Technologies) but with the addition of 20 mM HEPES. Images were collected using the 100× NA 1.4 Plan-Apochromat objective on the DeltaVision microscope. For each nucleus, 20 to 30 optical sections were recorded. The Hg lamp was attenuated with a 0.5 OD neutral density filter, and images were recorded using a binning of 3 × 3. Images were recorded every 10 min over a time period of 3 hr. Time-lapse images were viewed as 3D maximum intensity projections of each time point (SoftWoRx, Applied Precision, Inc.).

Photobleaching experiments were carried out on a ZEISS 510 confocal laser scanning microscope equipped with an argon-krypton laser (ZEISS). The 488 nm laser and a 63× plan Apolens with a 1.4 NA were used. A laser power of 2.5% was used in image acquisitions, and 25% was used for photobleaching. An area of 16 × 16 pixels was bleached with an iteration of 250 (duration of bleach was 3 s). An image was collected before and after every bleaching event, with 30 s intervals between each bleaching event.

Supplementary Material

The Supplementary Material contains two figures: (1) a diagram detailing the gene structure of human PSP1, including a representation of which exons are included in the major splice forms of PSP1, and (2) fluorescence micrographs showing that in HeLa cells treated with the transcription inhibitor Actinomycin D, YFP-p68 localizes to the same perinucleolar cap structure as PSP1. The Supplementary Material can be found at http://images.cellpress.com/supmat/supmatin.htm.

Acknowledgments

A.I.L. is a Wellcome Trust Principal Research Fellow and is funded by a Wellcome Trust Programme grant. A.H.F. is funded by a Wellcome Trust International Travelling Fellowship; A.K.L.L. is funded by a Croucher studentship; Y.W.L. is funded by a Croucher postdoctoral fellowship; and C.E.L. is funded by the Wellcome Trust. We would like to thank Dr. K. Collins for the 1787htert cell line. Work in M.M.'s laboratory is funded by a Danish National Research Foundation grant to the Centre for Experimental BioInformatics. We thank Dr. B. Frenguelli and Dr. C. Connolly from Ninewells Hospital, Dundee, for the use of the LSM510.

Received: October 15, 2001
Revised: November 14, 2001
Accepted: November 14, 2001
Published: January 8, 2002

References

1. Cremer, T., and Cremer, C. (2001). Chromosome territories, nuclear architecture and gene regulation in mammalian cells. Nat. Rev. Genet. *2*, 292–301.
2. Lamond, A.I., and Earnshaw, W.C. (1998). Structure and function in the nucleus. Science *280*, 547–553.
3. Pederson, T. (2001). Protein mobility within the nucleus—what are the right moves? Cell *104*, 635–638.
4. Misteli, T. (2001). Protein dynamics: implications for nuclear architecture and gene expression. Science *291*, 843–847.
5. Matera, A.G. (1999). Nuclear bodies: multifaceted subdomains of the interchromatin space. Trends Cell Biol. *9*, 302–309.
6. Weis, K., Rambaud, S., Lavau, C., Jansen, J., Carvalho, T., Carmo-Fonseca, M., Lamond, A., and Dejean, A. (1994). Retinoic acid regulates aberrant nuclear localization of PML-RAR alpha in acute promyelocytic leukemia cells. Cell *76*, 345–356.
7. Dyck, J.A., Maul, G.G., Miller, W.H., Jr., Chen, J.D., Kakizuka, A., and Evans, R.M. (1994). A novel macromolecular structure is a target of the promyelocyte-retinoic acid receptor oncoprotein. Cell *76*, 333–343.
8. Koken, M.H., Puvion-Dutilleul, F., Guillemin, M.C., Viron, A., Linares-Cruz, G., Stuurman, N., de Jong, L., Szostecki, C., Calvo, F., Chomienne, C., et al. (1994). The t(15;17) translocation alters a nuclear body in a retinoic acid-reversible fashion. EMBO J. *13*, 1073–1083.
9. Liu, Q., and Dreyfuss, G. (1996). A novel nuclear structure containing the survival of motor neurons protein. EMBO J. *15*, 3555–3565.
10. Bridge, E., Xia, D.X., Carmo-Fonseca, M., Cardinali, B., Lamond, A.I., and Pettersson, U. (1995). Dynamic organization of splicing factors in adenovirus-infected cells. J. Virol. *69*, 281–290.
11. Phelan, A., Carmo-Fonseca, M., McLaughlan, J., Lamond, A.I., and Clements, J.B. (1993). A herpes simplex virus type 1 immediate-early gene product, IE63, regulates small nuclear ribonucleoprotein distribution. Proc. Natl. Acad. Sci. USA *90*, 9056–9060.
12. Santama, N., Dotti, C.G., and Lamond, A.I. (1996). Neuronal differentiation in the rat hippocampus involves a stage-specific reorganization of subnuclear structure both in vivo and in vitro. Eur. J. Neurosci. *8*, 892–905.
13. Dahm, R., Gribbon, C., Quinlan, R.A., and Prescott, A.R. (1998). Changes in the nucleolar and coiled body compartments precede lamina and chromatin reorganization during fibre cell denucleation in the bovine lens. Eur. J. Cell Biol. *75*, 237–246.
14. Antoniou, M., Carmo-Fonseca, M., Ferreira, J., and Lamond, A.I. (1993). Nuclear organization of splicing snRNPs during differentiation of murine erythroleukemia cells in vitro. J. Cell Biol. *123*, 1055–1068.
15. Phair, R.D., and Misteli, T. (2000). High mobility of proteins in the mammalian cell nucleus. Nature *404*, 604–609.
16. Snaar, S., Wiesmeijer, K., Jochemsen, A.G., Tanke, H.J., and Dirks, R.W. (2000). Mutational analysis of fibrillarin and its mobility in living human cells. J. Cell Biol. *151*, 653–662.
17. Chen, D., and Huang, S. (2001). Nucleolar components involved in ribosome biogenesis cycle between the nucleolus and nucleoplasm in interphase cells. J. Cell Biol. *153*, 169–176.
18. Stenoien, D.L., Patel, K., Mancini, M.G., Dutertre, M., Smith, C.L., O'Malley, B.W., and Mancini, M.A. (2001). FRAP reveals that mobility of oestrogen receptor-alpha is ligand- and proteasome-dependent. Nat. Cell Biol. *3*, 15–23.
19. Spector, D.L., Fu, X.D., and Maniatis, T. (1991). Associations between distinct pre-mRNA splicing components and the cell nucleus. EMBO J. *10*, 3467–3481.
20. Carmo-Fonseca, M., Pepperkok, R., Carvalho, M.T., and Lamond, A.I. (1992). Transcription-dependent colocalization of the U1, U2, U4/U6, and U5 snRNPs in coiled bodies. J. Cell Biol. *117*, 1–14.
21. Carter, K.C., Bowman, D., Carrington, W., Fogarty, K., McNeil, J.A., Fay, F.S., and Lawrence, J.B. (1993). A three-dimensional view of precursor messenger RNA metabolism within the mammalian nucleus. Science *259*, 1330–1335.
22. Misteli, T., and Spector, D.L. (1998). The cellular organization of gene expression. Curr. Opin. Cell Biol. *10*, 323–331.

23. Dirks, R.W., Hattinger, C.M., Molenaar, C., and Snaar, S.P. (1999). Synthesis, processing, and transport of RNA within the three-dimensional context of the cell nucleus. Crit. Rev. Eukaryot. Gene Expr. *9*, 191–201.
24. Sleeman, J.E., and Lamond, A.I. (1999). Newly assembled snRNPs associate with coiled bodies before speckles, suggesting a nuclear snRNP maturation pathway. Curr. Biol. *9*, 1065–1074.
25. Speckmann, W., Narayanan, A., Terns, R., and Terns, M.P. (1999). Nuclear retention elements of U3 small nucleolar RNA. Mol. Cell. Biol. *19*, 8412–8421.
26. Yu, Y.T., Shu, M.D., Narayanan, A., Terns, R.M., Terns, M.P., and Steitz, J.A. (2001). Internal modification of u2 small nuclear (sn)rna occurs in nucleoli of xenopus oocytes. J. Cell Biol. *152*, 1279–1288.
27. Gall, J.G., Bellini, M., Wu, Z., and Murphy, C. (1999). Assembly of the nuclear transcription and processing machinery: Cajal bodies (coiled bodies) and transcriptosomes. Mol. Biol. Cell *10*, 4385–4402.
28. Frey, M.R., Bailey, A.D., Weiner, A.M., and Matera, A.G. (1999). Association of snRNA genes with coiled bodies is mediated by nascent snRNA transcripts. Curr. Biol. *9*, 126–135.
29. Pederson, T. (1998). The plurifunctional nucleolus. Nucleic Acids Res. *26*, 3871–3876.
30. Olson, M.O., Dundr, M., and Szebeni, A. (2000). The nucleolus: an old factory with unexpected capabilities. Trends Cell Biol. *10*, 189–196.
31. Carmo-Fonseca, M., Mendes-Soares, L., and Campos, I. (2000). To be or not to be in the nucleolus. Nat. Cell Biol. *2*, E107–112.
32. Andersen, J.S., Lyon, C.E., Fox, A.H., Leung, A.K.L., Lam, Y.W., Steen, H., Mann, M., and Lamond, A.I. (2002). Directed proteomic analysis of the human nucleolus. Curr. Biol. *12*, 1–11.
33. Dong, B., Horowitz, D.S., Kobayashi, R., and Krainer, A.R. (1993). Purification and cDNA cloning of HeLa cell p54nrb, a nuclear protein with two RNA recognition motifs and extensive homology to human splicing factor PSF and Drosophila NONA/BJ6. Nucleic Acids Res. *21*, 4085–4092.
34. Yang, Y.S., Hanke, J.H., Carayannopoulos, L., Craft, C.M., Capra, J.D., and Tucker, P.W. (1993). NonO, a non-POU-domain-containing, octamer-binding protein, is the mammalian homolog of Drosophila nonAdiss. Mol. Cell. Biol. *13*, 5593–5603.
35. Visa, N., Puvion-Dutilleul, F., Bachellerie, J.P., and Puvion, E. (1993). Intranuclear distribution of U1 and U2 snRNAs visualized by high resolution in situ hybridization: revelation of a novel compartment containing U1 but not U2 snRNA in HeLa cells. Eur. J. Cell Biol. *60*, 308–321.
36. Stuurman, N., de Graaf, A., Floore, A., Josso, A., Humbel, B., de Jong, L., and van Driel, R. (1992). A monoclonal antibody recognizing nuclear matrix-associated nuclear bodies. J. Cell Sci. *101*, 773–784.
37. Patton, J.G., Porro, E.B., Galceran, J., Tempst, P., and Nadal-Ginard, B. (1993). Cloning and characterization of PSF, a novel pre-mRNA splicing factor. Genes Dev. *7*, 393–406.
38. Lamm, G.M., Nicol, S.M., Fuller-Pace, F.V., and Lamond, A.I. (1996). p72: a human nuclear DEAD box protein highly related to p68. Nucleic Acids Res. *24*, 3739–3747.
39. Andrade, L.E., Chan, E.K., Raska, I., Peebles, C.L., Roos, G., and Tan, E.M. (1991). Human autoantibody to a novel protein of the nuclear coiled body: immunological characterization and cDNA cloning of p80-coilin. J. Exp. Med. *173*, 1407–1419.
40. Matunis, M.J., Michael, W.M., and Dreyfuss, G. (1992). Characterization and primary structure of the poly(C)-binding heterogeneous nuclear ribonucleoprotein complex K protein. Mol. Cell. Biol. *12*, 164–171.
41. Raska, I., Ochs, R.L., Andrade, L.E., Chan, E.K., Burlingame, R., Peebles, C., Gruol, D., and Tan, E.M. (1990). Association between the nucleolus and the coiled body. J. Struct. Biol. *104*, 120–127.
42. Ochs, R.L., Lischwe, M.A., Spohn, W.H., and Busch, H. (1985). Fibrillarin: a new protein of the nucleolus identified by autoimmune sera. Biol. Cell *54*, 123–133.
43. Mintz, P.J., Patterson, S.D., Neuwald, A.F., Spahr, C.S., and Spector, D.L. (1999). Purification and biochemical characterization of interchromatin granule clusters. EMBO J. *18*, 4308–4320.
44. Visintin, R., and Amon, A. (2000). The nucleolus: the magician's hat for cell cycle tricks. Curr. Opin. Cell Biol. *12*, 752.
45. Thiede, B., Dimmler, C., Siejak, F., and Rudel, T. (2001). Predominant identification of RNA-binding proteins in Fas-induced apoptosis by proteome analysis. J. Biol. Chem. *276*, 26044–26050.
46. Hallier, M., Tavitian, A., and Moreau-Gachelin, F. (1996). The transcription factor Spi-1/PU.1 binds RNA and interferes with the RNA-binding protein p54nrb. J. Biol. Chem. *271*, 11177–11181.
47. Basu, A., Dong, B., Krainer, A.R., and Howe, C.C. (1997). The intracisternal A-particle proximal enhancer-binding protein activates transcription and is identical to the RNA- and DNA-binding protein p54nrb/NonO. Mol. Cell. Biol. *17*, 677–686.
48. Yang, Y.S., Yang, M.C., Tucker, P.W., and Capra, J.D. (1997). NonO enhances the association of many DNA-binding proteins to their targets. Nucleic Acids Res. *25*, 2284–2292.
49. Zhang, Z., and Carmichael, G.G. (2001). The fate of dsRNA in the nucleus: a p54(nrb)-containing complex mediates the nuclear retention of promiscuously A-to-I edited RNAs. Cell *106*, 465–475.
50. Mathur, M., Tucker, P.W., and Samuels, H.H. (2001). PSF is a novel corepressor that mediates its effect through Sin3A and the DNA binding domain of nuclear hormone receptors. Mol. Cell. Biol. *21*, 2298–2311.
51. Iwasaki, T., Chin, W.W., and Ko, L. (2001). Identification and characterization of rrm-containing coactivator activator (coaa) as trbp-interacting protein, and its splice variant as a coactivator modulator (coam). J. Biol. Chem. *276*, 33375–33383.
52. Dye, B.T., and Patton, J.G. (2001). An RNA recognition motif (RRM) is required for the localization of PTB-associated splicing factor (PSF) to subnuclear speckles. Exp. Cell Res. *263*, 131–144.
53. Miralles, F., Ofverstedt, L.G., Sabri, N., Aissouni, Y., Hellman, U., Skoglund, U., and Visa, N. (2000). Electron tomography reveals posttranscriptional binding of pre-mRNPs to specific fibers in the nucleoplasm. J. Cell Biol. *148*, 271–282.
54. Chiodi, I., Biggiogera, M., Denegri, M., Corioni, M., Weighardt, F., Cobianchi, F., Riva, S., and Biamonti, G. (2000). Structure and dynamics of hnRNP-labelled nuclear bodies induced by stress treatments. J. Cell Sci. *113*, 4043–4053.
55. Weighardt, F., Cobianchi, F., Cartegni, L., Chiodi, I., Villa, A., Riva, S., and Biamonti, G. (1999). A novel hnRNP protein (HAP/SAF-B) enters a subset of hnRNP complexes and relocates in nuclear granules in response to heat shock. J. Cell Sci. *112*, 1465–1476.
56. Prasanth, K.V., Rajendra, T.K., Lal, A.K., and Lakhotia, S.C. (2000). Omega speckles—a novel class of nuclear speckles containing hnRNPs associated with noncoding hsr-omega RNA in Drosophila. J. Cell Sci. *113*, 3485–3497.
57. Elefanty, A.G., Antoniou, M., Custodio, N., Carmo-Fonseca, M., and Grosveld, F.G. (1996). GATA transcription factors associate with a novel class of nuclear bodies in erythroblasts and megakaryocytes. EMBO J. *15*, 319–333.
58. Saurin, A.J., Shiels, C., Williamson, J., Satijn, D.P., Otte, A.P., Sheer, D., and Freemont, P.S. (1998). The human polycomb group complex associates with pericentromeric heterochromatin to form a novel nuclear domain. J. Cell Biol. *142*, 887–898.
59. Cotto, J., Fox, S., and Morimoto, R. (1997). HSF1 granules: a novel stress-induced nuclear compartment of human cells. J. Cell Sci. *110*, 2925–2934.
60. Chen, T., Boisvert, F.M., Bazett-Jones, D.P., and Richard, S. (1999). A role for the GSG domain in localizing Sam68 to novel nuclear structures in cancer cell lines. Mol. Biol. Cell *10*, 3015–3033.
61. Nayler, O., Hartmann, A.M., and Stamm, S. (2000). The ER repeat protein YT521-B localizes to a novel subnuclear compartment. J. Cell Biol. *150*, 949–962.
62. Huang, S. (2000). Review: perinucleolar structures. J. Struct. Biol. *129*, 233–240.
63. Green, S., Issemann, I., and Sheer, E. (1988). A versatile in vivo and in vitro eukaryotic expression vector for protein engineering. Nucleic Acids Res. *16*, 369.
64. Sleeman, J., Ajuh, P., and Lamond, A.I. (2001). snRNP protein

expression enhances the formation of Cajal bodies containing p80-Coilin and SMN. J. Cell Sci., in press.
65. Platani, M., Goldberg, I., Swedlow, J.R., and Lamond, A.I. (2000). In vivo analysis of Cajal body movement, separation, and joining in live human cells. J. Cell Biol. *151*, 1561–1574.
66. Reimer, G., Raska, I., Tan, E.M., and Scheer, U. (1987). Human autoantibodies: probes for nucleolus structure and function. Virchows Arch. B Cell Pathol. Incl. Mol. Pathol. *54*, 131–143.
67. Evan, G.I., Lewis, G.K., Ramsay, G., and Bishop, J.M. (1985). Isolation of monoclonal antibodies specific for human c-myc proto-oncogene product. Mol. Cell. Biol. *5*, 3610–3616.
68. Masson, C., Bouniol, C., Fomproix, N., Szollosi, S., Debey, P., and Hernandez-Verdun, D. (1996). Conditions favouring RNA polymerase I transcription in permeabilized cells. Exp. Cell Res. *226*, 114–125.

Accession Numbers

The GenBank accession numbers for PSP1-α and PSP1-β have been deposited as AF448795 and AF449627, respectively.